

AD-752 540

PULSED-POWER BURNOUT OF INTEGRATED
CIRCUITS

R. H. Vandre

Aerospace Corporation

Prepared for:

Air Force Systems Command

15 August 1972

DISTRIBUTED BY:



National Technical Information Service
U. S. DEPARTMENT OF COMMERCE
5285 Port Royal Road, Springfield Va. 22151

AD752540

Pulsed-Power Burnout of Integrated Circuits

Prepared by R. H. VANDRE
Plasma Research Laboratory
Laboratory Operations

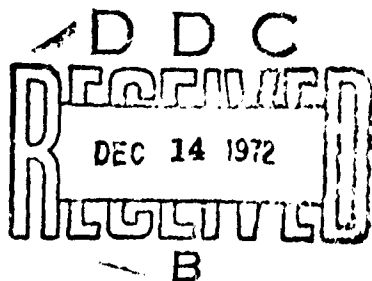
72 AUG 15

Technology Division
THE AEROSPACE CORPORATION

Prepared for SPACE AND MISSILE SYSTEMS ORGANIZATION
AIR FORCE SYSTEMS COMMAND
LOS ANGELES AIR FORCE STATION
Los Angeles, California

Reproduced by
NATIONAL TECHNICAL
INFORMATION SERVICE
U.S. Department of Commerce
Springfield VA 22161

APPROVED FOR PUBLIC RELEASE:
DISTRIBUTION UNLIMITED



LABORATORY OPERATIONS

The Laboratory Operations of The Aerospace Corporation is conducting experimental and theoretical investigations necessary for the evaluation and application of scientific advances to new military concepts and systems. Versatility and flexibility have been developed to a high degree by the laboratory personnel in dealing with the many problems encountered in the nation's rapidly developing space and missile systems. Expertise in the latest scientific developments is vital to the accomplishment of tasks related to these problems. The laboratories that contribute to this research are:

Aerodynamics and Propulsion Research Laboratory: Launch and reentry aerodynamics, heat transfer, reentry physics, propulsion, high-temperature chemistry and chemical kinetics, structural mechanics, flight dynamics, atmospheric pollution, and high-power gas lasers.

Electronics Research Laboratory: Generation, transmission, detection, and processing of electromagnetic radiation in the terrestrial and space environments, with emphasis on the millimeter-wave, infrared, and visible portions of the spectrum; design and fabrication of antennas, complex optical systems and photolithographic solid-state devices; test and development of practical superconducting detectors and laser devices and technology, including high-power lasers, atmospheric pollution, and biomedical problems.

Materials Sciences Laboratory: Development of new materials; metal matrix composites and new forms of carbon; test and evaluation of graphite and ceramics in reentry; spacecraft materials and components in radiation and high-vacuum environments; application of fracture mechanics to stress corrosion and fatigue-induced fractures in structural metals; effect of nature of material surfaces on lubrication, photosensitization, and catalytic reactions, and development of prosthesis devices.

Plasma Research Laboratory: Reentry physics and nuclear weapons effects; the interaction of antennas with reentry plasma sheaths; experimentation with thermonuclear plasmas; the generation and propagation of plasma waves in the magnetosphere; chemical reactions of vibrationally excited species in rocket plumes; and high-precision laser ranging.

Space Physics Laboratory: Aeronomy; density and composition of the atmosphere at all altitudes; atmospheric reactions and atmospheric optics; pollution of the environment; the sun, earth's resources; meteorological measurements; radiation belts and cosmic rays; and the effects of nuclear explosions, magnetic storms, and solar radiation on the atmosphere.

THE AEROSPACE CORPORATION
El Segundo, California

ACCESSION FOR	
RTS	WHITE Sheets <input checked="" type="checkbox"/>
D/C	Black Sheets <input type="checkbox"/>
24. 10. 1984	<input type="checkbox"/>
24. 10. 1984	<input type="checkbox"/>
DATE AVAILABLE FOR USE	
10. 10. 1984	
REMARKS	
A	

UNCLASSIFIED

Security Classification

DOCUMENT CONTROL DATA - R & D

(Security classification of title, body of abstract and indexing annotation must be entered when the overall report is classified)

1. ORIGINATING ACTIVITY (Corporate author) The Aerospace Corporation El Segundo, California	2a REPORT SECURITY CLASSIFICATION Unclassified
	2b GROUP

3. REPORT TITLE

Pulsed-Power Burnout of Integrated Circuits

4 DESCRIPTIVE NOTES (Type of report and inclusive dates)

5 AUTHOR(S) (First name, middle initial, last name)

Robert H. Vandre

6 REPORT DATE 72 AUG 15	7a TOTAL NO. OF PAGES 38 42	7b NO. OF REFS 1
8a CONTRACT OR GRANT NO. F04701- 72-C-0073	9a ORIGINATOR'S REPORT NUMBER(S) TR-0073(3124)-1	
b PROJECT NO.		
c	9b OTHER REPORT NO(S) (Any other numbers that may be assigned this report)	
d	SAMSO-TR-72-226	

10. DISTRIBUTION STATEMENT

Approved for public release; distribution unlimited.

11. SUPPLEMENTARY NOTES	12. SPONSORING MILITARY ACTIVITY Space and Missile Systems Organization Air Force Systems Command Los Angeles Air Force Station
-------------------------	--

13. ABSTRACT

Results of pulsed-power burnout testing the Fairchild 9046 quad dual-input nand gate and the Amelco 6041 three-input nand gate showed the circuits to be vulnerable to junction burnout for pulses of less than 100 V and pulse widths on the order of 100 nsec. Calculations based on Wunsch-Bell junction burnout theory showed good agreement with the experimental results. Sample calculations applying Wunsch-Bell theory to integrated circuits are given.

UNCLASSIFIED

Security Classification

14

KEY WORDS

EMP

Integrated circuit pulse burnout

Junction burnout

Wunsch-Bell theory

Distribution Statement (Continued)

Abstract (Continued)

1b

UNCLASSIFIED

Security Classification

Air Force Report No.
SAMSC-TR-72-226

Aerospace Report No.
TR-0073(3124)-1

PULSED-POWER BURNOUT OF INTEGRATED CIRCUITS

Prepared by
R. H. Vandre
Plasma Research Laboratory
Laboratory Operations

72 AUG 15

Technology Division
THE AEROSPACE CORPORATION

Prepared for
SPACE AND MISSILE SYSTEMS ORGANIZATION
AIR FORCE SYSTEMS COMMAND
LOS ANGELES AIR FORCE STATION
Los Angeles, California

Approved for public release;
distribution unlimited.

ic

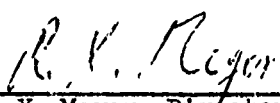
FOREWORD

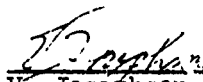
This report is published by The Aerospace Corporation, El Segundo, California, under Air Force Contract No. F04701-72-J-0073.

This report, which documents research carried out from September 1971 through March 1972, was submitted on 15 August 1972 to Major James H. Heilman, DYX, for review and approval.

The author is grateful to Dr. V. Josephson for his encouragement and support during the course of this work and to R. Marshall for his technical support.

Approved


R. X. Meyer, Director
Plasma Research Laboratory
Laboratory Operations


V. Josephson, Associate Group
Director
Development and Survivability
Directorate
Technology Division

Publication of this report does not constitute Air Force approval of the report's findings or conclusions. It is published only for the exchange and stimulation of ideas.


James H. Heilman, Major, USAF
Survivability Directorate

ABSTRACT

Results of pulsed-power burnout testing of the Fairchild 9046 quad dual-input nand gate and the Amelco 6041 dual three-input nand gate showed the circuits to be vulnerable to junction burnout for pulses of less than 100 V and pulse widths on the order of 100 nsec. Calculations based on Wunsch-Bell junction burnout theory showed good agreement with the experimental results. Sample calculations applying Wunsch-Bell theory to integrated circuits are given.

CONTENTS

FOREWORD	ii
ABSTRACT	iii
I. INTRODUCTION	1
II. WUNSCH-BELL THEORY	3
III. EXPERIMENTAL APPARATUS	7
A. Test Setup	7
B. Experimental Procedure	7
IV. RESULTS AND CONCLUSIONS	11
Table 1. Burnout Voltages	10
APPENDIX A. WUNSCH-BELL CALCULATIONS FOR A PULSE APPLIED TO THE OUTPUT OF THE FAIRCHILD 9046 NAND GATE	19
APPENDIX B. WUNSCH-BELL CALCULATIONS FOR A PULSE ON THE INPUT OF AN AMELCO 6041 NAND GATE	27

Preceding page blank

FIGURES

1.	Wunsch-Bell Burnout Limits for Silicon	4
2.	Experimental Setup	6
3.	Pulses from High-Power Pulser	8
4.	Comparison of Wunsch-Bell Theory and Experiment for Fairchild 9046 Nand Gate with Positive Pulse on Input with Other Input at Ground	12
5.	Comparison of Wunsch-Bell Theory and Experiment for Fairchild 9046 Nand Gate with Positive Pulse on Output.	13
6.	Comparison of Wunsch-Bell Theory and Experiment for Amelco 6041 Nand Gate with Negative Pulse on Input	14
7.	Comparison of Wunsch-Bell Theory and Experiment for Amelco 6041 Nand Gate with Positive Pulse on Input	15
8.	Comparison of Wunsch-Bell Theory and Experiment for Amelco 6041 Nand Gate with Positive and Negative Pulses on Output	16
9.	Circuit Diagram for One Channel of the Fairchild 9046 Quad Dual-Input Nand Gate	18
10.	Output Transistor Geometry of Fairchild 9046 Quad Dual-Input Nand Gate	20
11.	The Three Contributions to the Bulk Resistance of a Transistor	22
12.	Sample Calculation of Number of "Squares"	22
13.	Power Dissipated Across Junction of Output Transistor of Amelco 6041 Dual Three-Input Nand Gate with High-Power Pulser on Output Connection	24
14.	Photomicrograph of Burned-Out Fairchild 9046 Output Transistor Caused by Pulses Applied to Output	25
15.	Circuit Diagram for One Channel of Amelco 6041 Dual Three-Input Nand Gate	28

Preceding page blank

FIGURES (Concluded)

- | | | |
|-----|--|----|
| 16. | Photomicrograph of Amelco 6041 Nand Gate Geometry | 29 |
| 17. | Power Dissipated at Emitter Junction of Transistor T1 or
T2 of Amelco 6041 Nand Gate with Negative High-Power
Pulses on Input | 31 |
| 18. | Photomicrograph of Amelco 6041 Nand Gate After Application
of High-Power Negative Pulse to Input, Showing Failure of
Transistors T1 and T2 | 32 |
| 19. | Photomicrograph of Amelco 6041 Nand Gate After Application
of High-Power Negative Pulse to Input, Showing Failure of
Diode D1 and Transistors T1, T2, and T3 | 33 |

I. INTRODUCTION

An important long-range mechanism by which satellite electronics can be adversely affected is the electromagnetic pulse (EMP) associated with nuclear detonations occurring above the atmosphere. This pulse can couple directly into the satellite antennas proper or, through slots in the satellite structure, into unshielded wires leading directly to electronics boxes. The magnitude of the voltage transients generated in the electronics and the hardness of the electronics determine the vulnerability of the electronics to burnout. The theoretical model used in prediction of semiconductor junction burnout voltages is that developed by Wunsch and Bell.¹ This theory predicts the power level per unit area for a given pulse width necessary to heat a semiconductor junction to the melting point of silicon. Extensive tests were conducted by Wunsch and Bell on discrete transistors and diodes, and agreement was obtained with the theory. A major conclusion of their work was that burnout comes at a power level between that predicted by theory and a level one tenth as high. This result is explained by photomicrographs of the semiconductor junctions, which showed that melting of the junction usually occurred at isolated spots that covered only a fraction of the junction area.

¹D. L. Wunsch and R. R. Bell, "Determination of Threshold Failure Levels of Semiconductor Diodes and Transistors Due to Pulsed Voltages," IEEE Trans. Nucl. Sci. NS-15, 244 (1968).

Wunsch-Bell theory is used extensively to predict the burnout levels of discrete components but is seldom used on integrated circuits because of the difficulty involved in determination of device parameters, such as junction area and doping levels. This report is an account of measurements of EMP burnout levels for two integrated circuits, the Fairchild 9046 quad dual-input nand gate and the Amelco 6041 dual three-input nand gate. These circuits utilize standard low-power Transistor-Transistor Logic (TTL) design techniques and are used extensively in spacecraft because of their low power consumption (~ 1 mW). Because of their function, these circuits are used in positions in spacecraft where they are subjected to the EMP environment. This report presents experimental data and Wunsch-Bell predictions of the burnout levels for comparison purposes. Sample calculations and a comparison between the Wunsch-Bell theory and experimental values are included.

II. WUNSCH-BELL THEORY

Wunsch-Bell theory can be a useful tool for prediction of burnout of integrated circuits. To use it effectively, one must make an accurate estimate of the power dissipated in the vicinity of the semiconductor junction under consideration.

The Wunsch-Bell burnout model predicts the pulsed power level per unit area necessary to raise a semiconductor junction to the melting temperature. It is assumed that when the junction reaches this temperature it will fail. The model uses linear heat-flow theory to derive the following junction failure relation²

$$\frac{P}{A} = \sqrt{\pi k \rho c_p} [T_m - T_i] t^{-1/2}$$

where P is the power, A the junction area, k the thermal conductivity, ρ the density, c_p the specific heat, T_m the failure temperature, T_i the initial temperature, and t the time. Figure 1 is a graph of P vs A for silicon at room temperature.

The value of P to be used in the above equation must be determined with care. Only power dissipated in the immediate vicinity of the junction will contribute toward raising its temperature to the melting point. Power is dissipated in a semiconductor device either (1) across the junction itself

$$P = IV$$

where V is either the forward voltage drop or the reverse breakdown voltage, depending on the polarity of the pulse; or (2) in the bulk resistance R_{BULK}

² See Footnote 1.

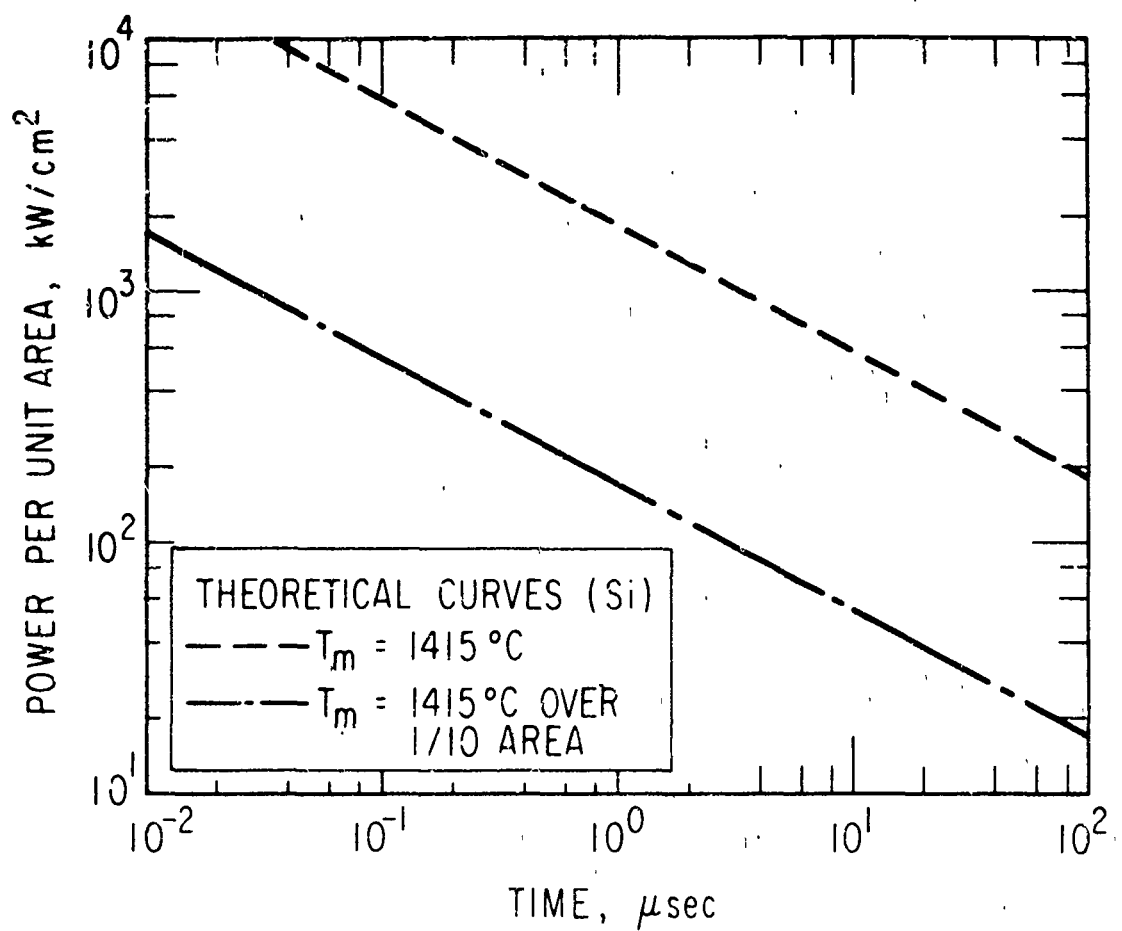


Figure 1. Wunsch-Bell Burnout Limits for Silicon

of the device

$$P = I^2 R_{BULK}$$

Power dissipated across the junction should clearly be included in calculation of burnout by the Wunsch-Bell theory. The situation is not so clear with regard to power dissipated in the bulk resistance. For current flowing from emitter to collector, most of the bulk resistance is in the collector and, therefore, far away from the junction. In this situation one would not include the $P = I^2 R_{BULK}$ term. Conversely, if one were considering a current path from base to emitter or base to collector, the $P = I^2 R_{BULK}$ term (R_{BULK} is the bulk resistance of the base) should usually be included. For a more complete explanation of the application of Wunsch-Bell theory to circuits, see Appendix A.

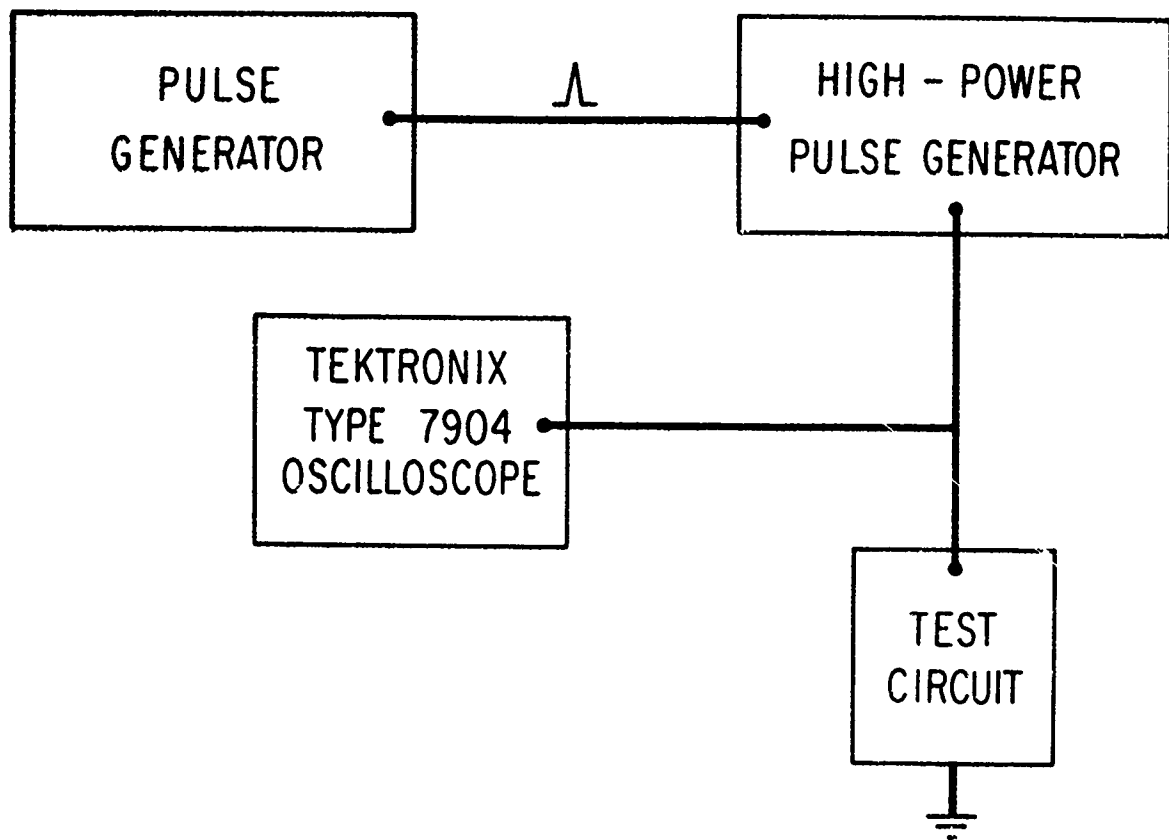


Figure 2. Experimental Setup

III. EXPERIMENTAL APPARATUS

A. TEST SETUP

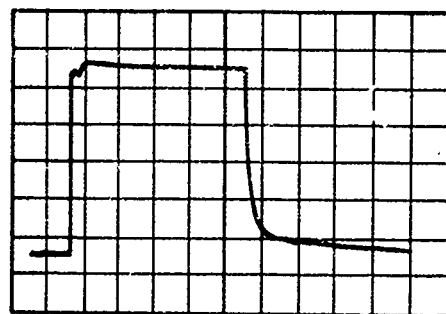
The basic electrical test setup is shown in Figure 2. A single-pulse generator was used to trigger the high-power pulser. The pulse from the high-power pulser was then fed into the test circuit and measured by a Tektronix 7904 oscilloscope (the risetime of the scope and amplifier is 0.8 nsec).

The high-power pulser used five MPSU 04 transistors avalanched in series to obtain square pulses of from 100 to 450 V across 50Ω with a risetime of approximately 1 nsec. For longer pulses of lower voltage, an emitter follower circuit with a TIP 33A power transistor was used to amplify an input square pulse. Pulses with amplitudes ranging from 1 to 60 V (across as little as 10Ω) and with risetimes of approximately 80 nsec were obtained.

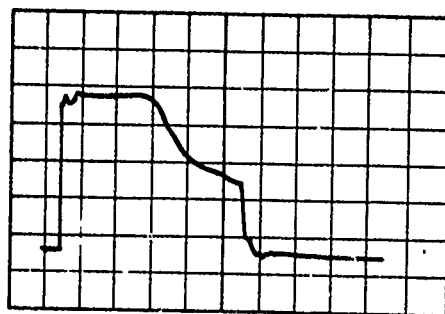
B. EXPERIMENTAL PROCEDURE

Each device was thoroughly checked for performance before burnout testing was initiated. After each high-power pulse, the device was tested for failure, which consisted of either a change in risetime or a change in logic voltage. The pulses started at low voltage and increased until failure occurred. After a failure had occurred, the cover was taken off the chip and a photomicrograph was made to determine the type of damage mechanism.

A typical pulse without a load can be seen in Figure 3a. Figure 3b shows the same pulse across an integrated circuit under test. Note that the maximum amplitude of the pulse across the test circuit is lower than the amplitude of the unloaded pulse. This happens because the circuit under



a. Unloaded Pulse



b. Pulse Across Integrated Circuit

Figure 3. Pulses from High-Power Pulser

test tends to load down the pulser. Figure 3b shows that, after ~40 nsec, the integrated circuit breaks down and loads the pulser even more.

In the calculations on the basis of the Wunsch-Bell model a constant voltage across the device for the duration of the pulse was assumed. Accordingly, the voltage reported for burnout is the average voltage across the junction during the high-power pulse. In most cases the peak voltage was ~40 to 50 percent higher.

Table 1. Burnout Voltages

Fairchild 9046 Quad Dual-Input Nand Gate					
Pulse On	Pulse Width, nsec	Average Pulse, V	Wunsch-Bell Total Junction Predicted	Melt, V	Failure Mode
Power supply	100	+400	700	700	Metallization burnout
Input (with other input at ground)	60 110 125	+105 +95 +100	150 125 120	150 125 120	Input diode burnout Input diode burnout Input diode burnout
Input (with other input floating)	25 100 640	-120 -100 -65	250 150 85	250 150 85	Inner transistor burnout Inner transistor burnout Inner transistor and input diode burnout
Output	25 60 100 640	+115 +58 +48 +34	200 140 110 50	200 140 110 50	Output transistor burnout Output transistor burnout Output transistor burnout Output transistor burnout
Amelco 6041 Dual Three-Input Nand Gate					
Pulse On	Pulse Width, nsec	Average Pulse, V	Wunsch-Bell Total Junction Predicted	Melt, V	Failure Mode
Input (with other input floating)	25 100	115 +72	350 210	350 210	Inner transistor and input diode burnout Inner transistor and input diode burnout
Output	25 100 1500 11,000	+72 +30 +35 +25	430 230 77 34	430 230 77 34	Metallization burnout Output transistor burnout Output transistor burnout Output transistor burnout

IV. RESULTS AND CONCLUSIONS

The results of pulsed voltage testing of the Fairchild 9046 quad dual-input nand gate and the Amelco 6041 dual three-input nand gate showed good agreement with Wunsch-Bell theory. In almost all cases, the voltage required for junction burnout lay between the 1/10 junction melt and total junction melt curves. Photomicrographs of the burned-out circuits showed that, in all but two instances, junction burnout occurred. In the two isolated instances, metallization burnout was the cause of failure.

A list of the devices tested and their burnout voltages is given in Table 1. In addition, Wunsch-Bell calculations for the different test configurations were performed. The results of these calculations can be seen in Figures 4-8.

Comparisons of experimental data and Wunsch-Bell theory show good agreement when the theory is extended to integrated circuits. The results also show that burnout almost always occurs at a level greater than the 1/10 junction melt level. Therefore, one could use Wunsch-Bell calculations in actual practice to see which circuits of a system under study might be stressed to the 1/10 junction melt level, and the exact burnout levels of these circuits could be determined by bench testing.

The difficulty of using Wunsch-Bell theory for integrated circuits is in the determination of necessary parameters for calculation: the resistivity of the collector, the base sheet resistance, the buried layer sheet resistance, the depth of the buried layer, the depth of the emitter,

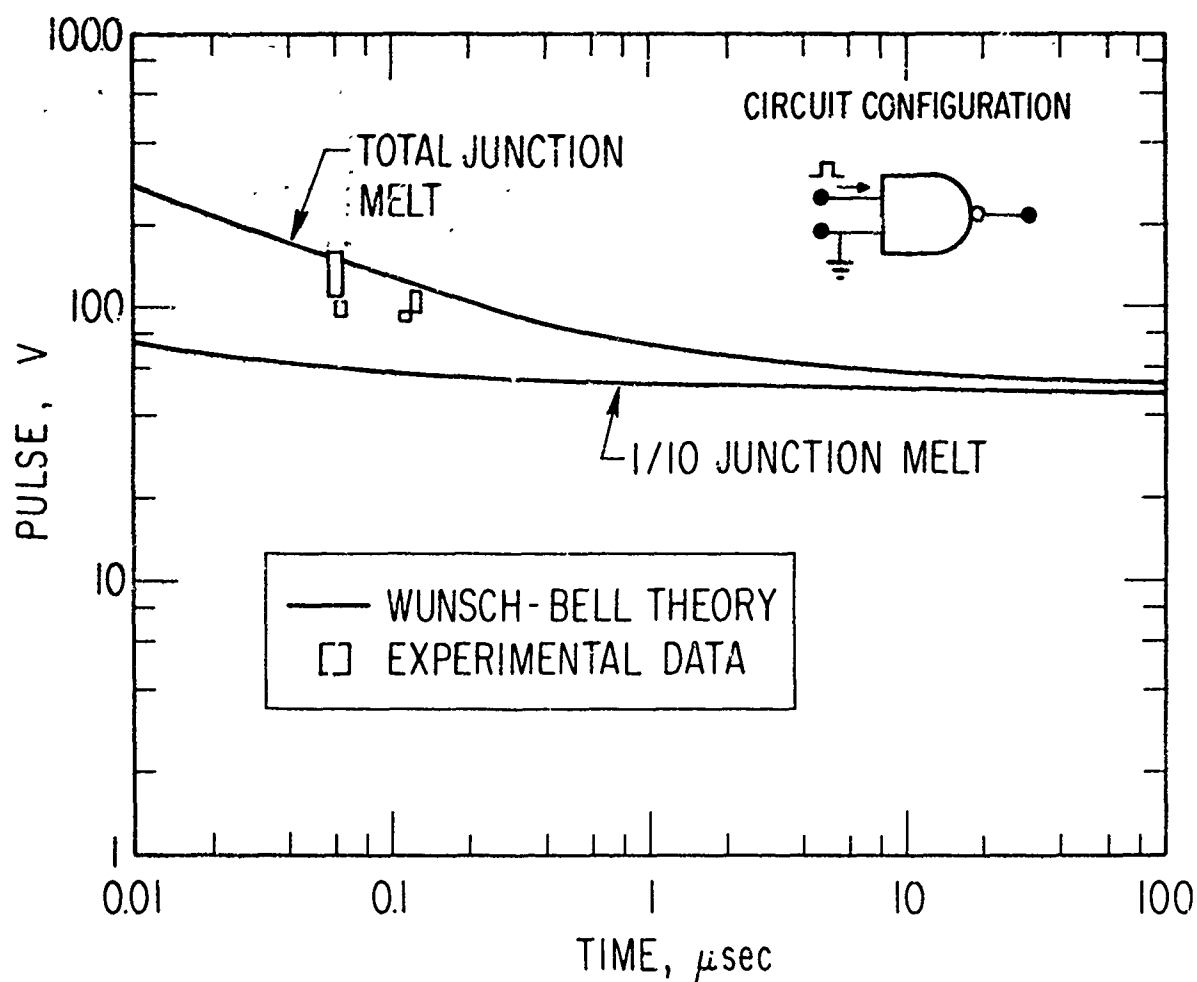


Figure 4. Comparison of Wunsch-Bell Theory and Experiment
for Fairchild 9046 Nand Gate with Positive Pulse
on Input with Other Input at Ground

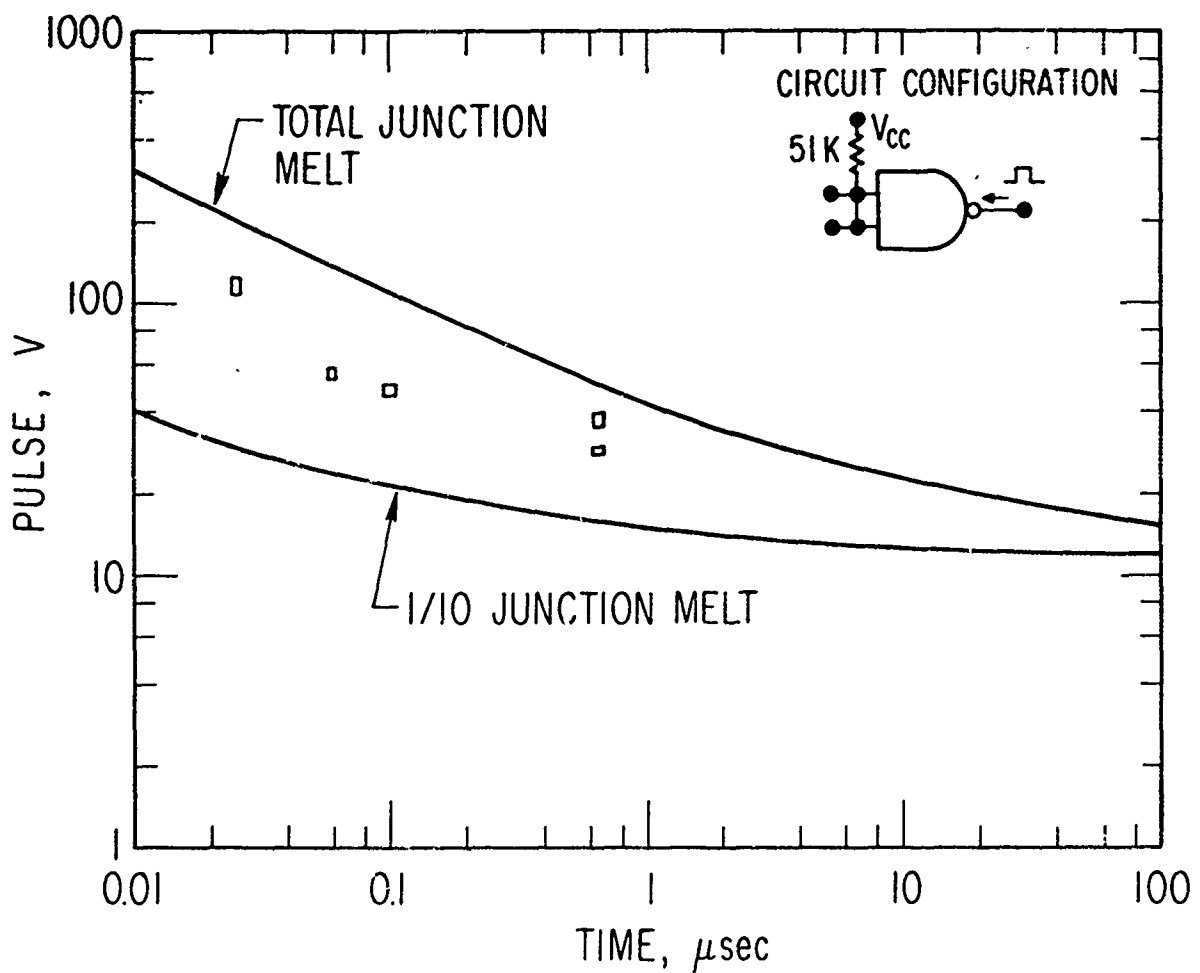


Figure 5. Comparison of Wunsch-Bell Theory and Experiment
for Fairchild 9046 Nand Gate with Positive
Pulse on Output

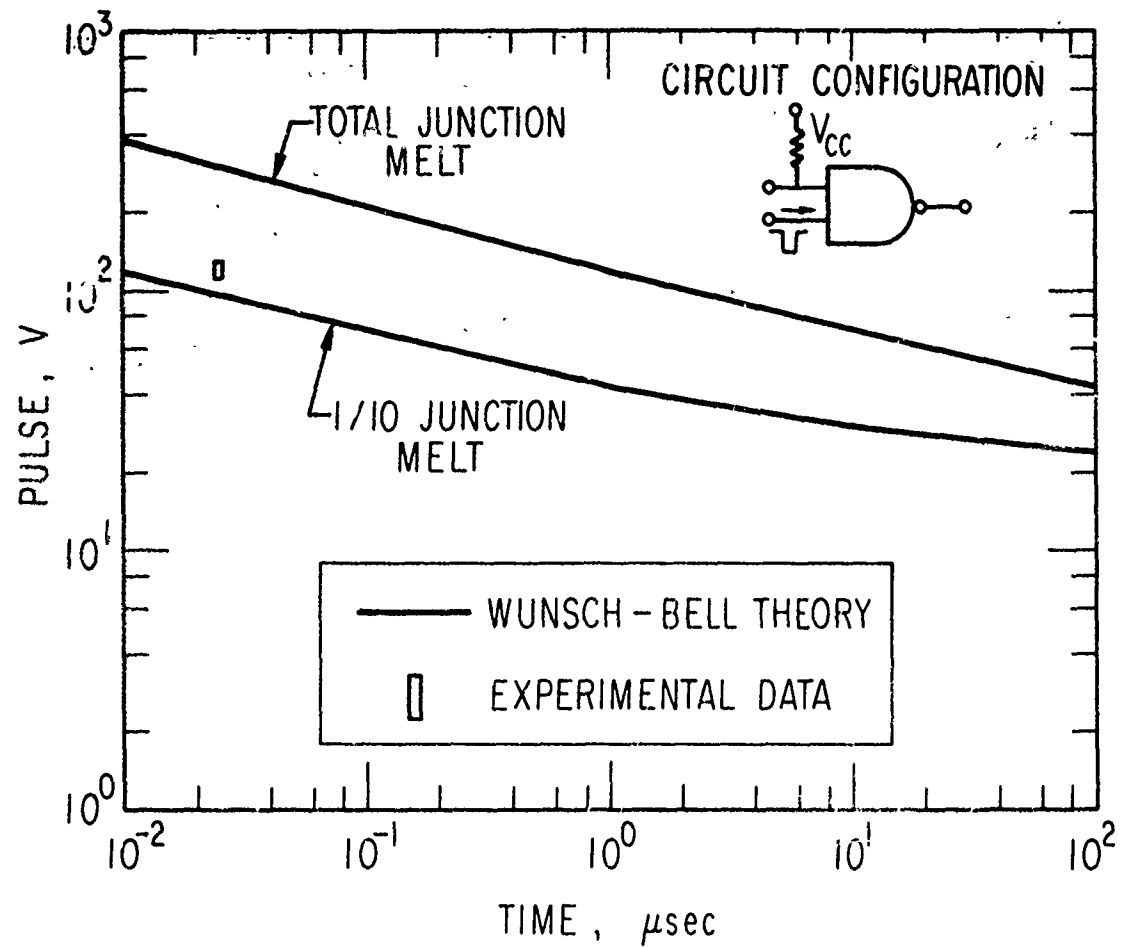


Figure 6. Comparison of Wunsch-Bell Theory and Experiment for
Amelco 6041 Nand Gate with Negative Pulse
on Input

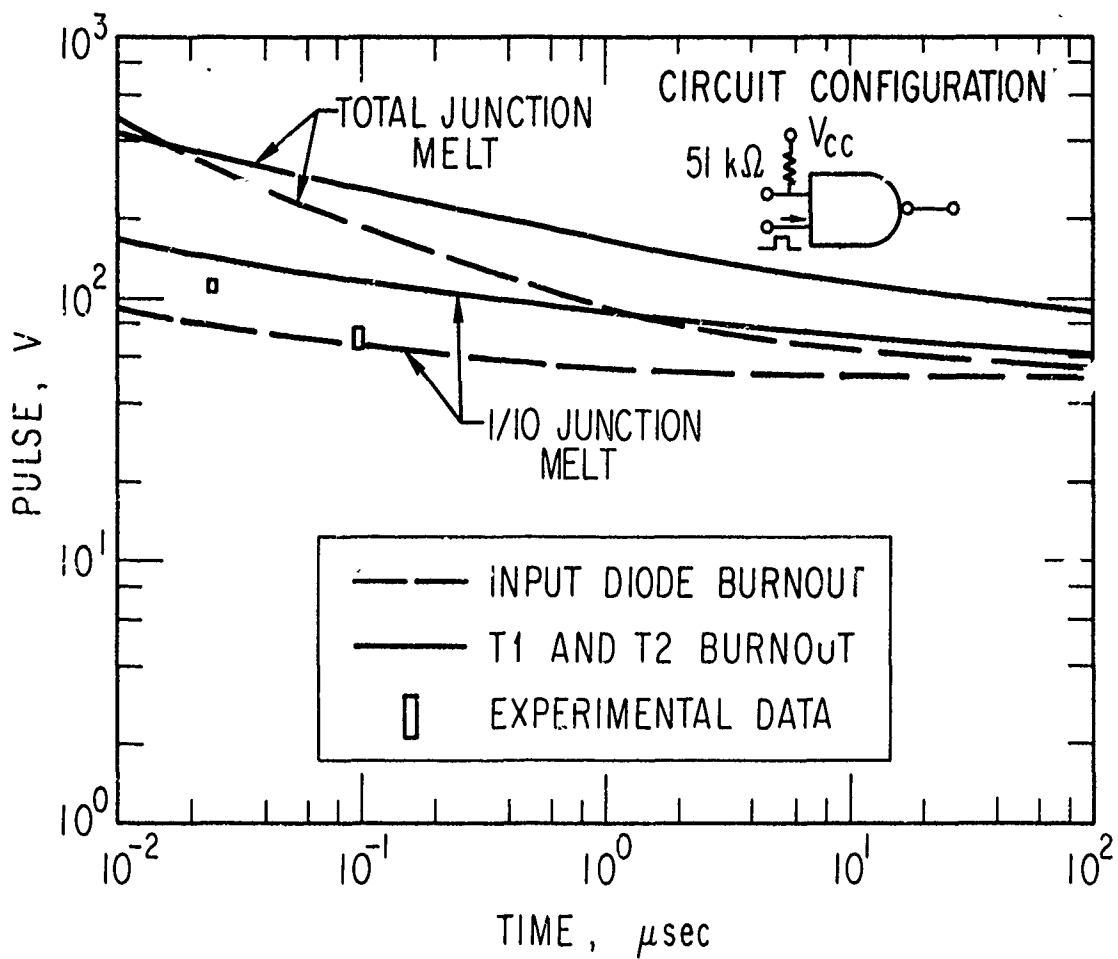


Figure 7. Comparison of Wunsch-Bell Theory and Experiment for Amelco 6041 Nand Gate with Positive Pulse on Input

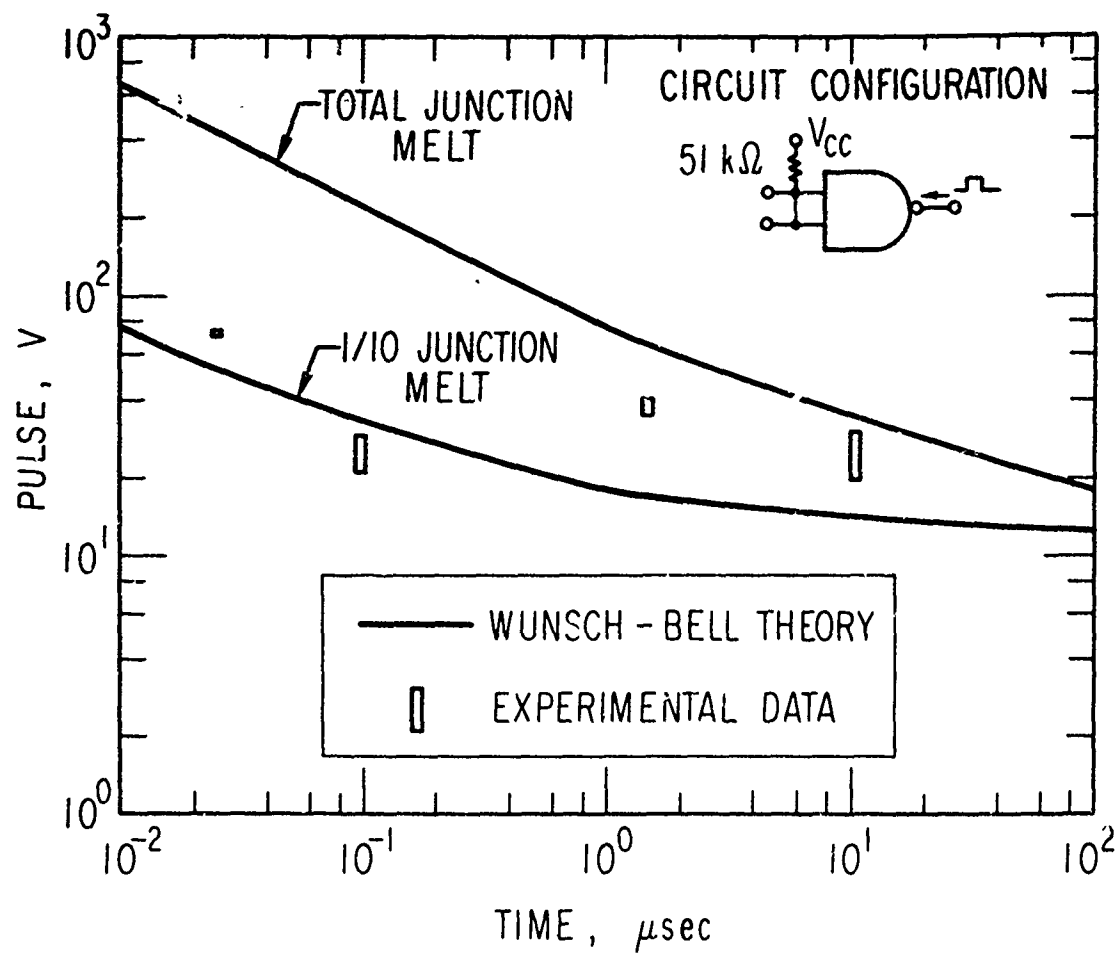
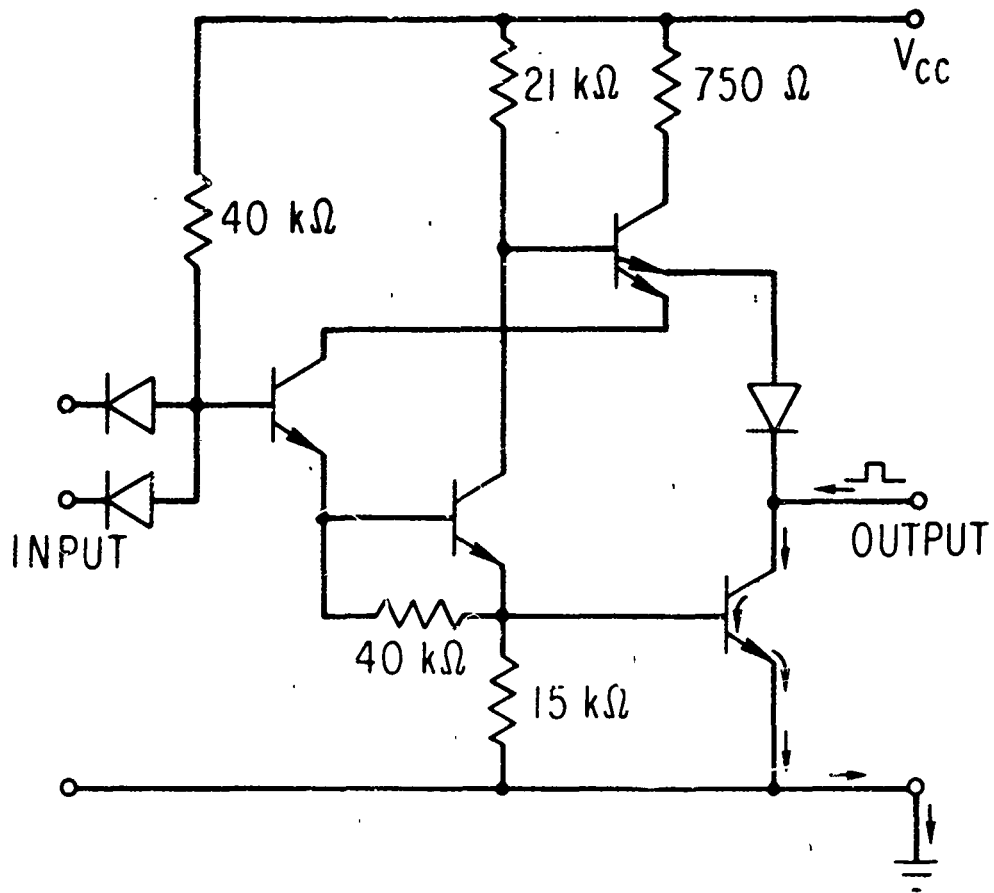


Figure 8. Comparison of Wunsch-Bell Theory and Experiment for Amelco 6041 Nand Gate with Positive and Negative Pulses on Output

the depth of the base, and the junction areas. Once these parameters are determined, the calculations are straightforward. Sample Wunsch-Bell calculations are given in Appendix A.



CIRCUIT CHARACTERISTICS

BV_{CEO} = 8 V MIN.; 12-15 V TYPICAL

BV_{EBO} = 6 V MIN.; 7-8 V TYPICAL

BV_{CBO} = 40 V MIN.; 50 V TYPICAL

ρ_c = 0.2 Ω - cm

R_{BURIED} = 3 Ω / SQUARE
LAYER

Figure 9. Circuit Diagram for One Channel of the Fairchild 9046 Quad Dual-Input Nand Gate

APPENDIX A. WUNSCH-BELL CALCULATIONS FOR A PULSE APPLIED
TO THE OUTPUT OF THE FAIRCHILD 9046 NAND GATE

The circuit diagram is shown in Figure 9. Because of the resistors going up to the power supply, the main current path is through the output transistor. The geometry of the output transistor is shown in Figure 10. Calculations of burnout of a specific active element depend on the ability of the power dissipated in the bulk resistance to add to heating effects at the junction. In the case of the output transistor, most of the bulk resistance is located in the collector. Therefore, most of the power dissipated in the bulk resistance of the device is too far removed from the junction to cause significant heating of the junction during a short pulse. The power dissipated at the junction is therefore

$$P = IV \quad (A.1)$$

where V is the voltage drop across the transistor. It is obvious that this V term will be largest when the junction is broken down in the reverse direction. In this case, large currents can be drawn that are limited only by the sum of the bulk resistance and metallization resistance of the device.

Figure 9 shows that, for a current path going through the output transistor, where the transistor is broken down in the reverse direction, the current is

$$I = (V - BV_{CEO})/R_T \quad (A.2)$$

The difficulty in application of Wunsch-Bell theory is the determination of the value for the bulk resistance. Because it is usually impossible

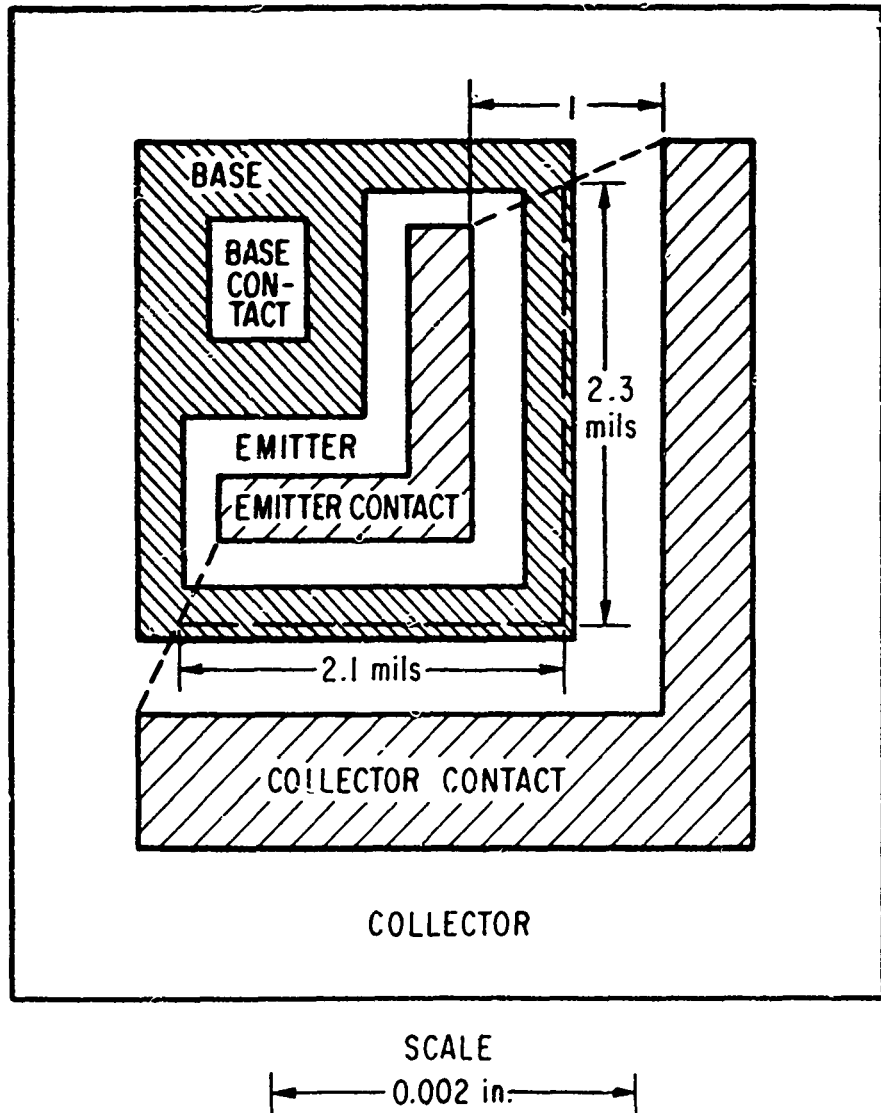


Figure 10. Output Transistor Geometry of Fairchild 9046 Quad Dual-Input Nand Gate

to measure bulk resistance in integrated circuits, and because the manufacturers usually don't supply information on such parameters, it is necessary to calculate these resistances. The resistance of the device is broken down into three components, which are shown in Figure 11.

The up-down resistance (R_{UD}) and the down-up resistance (R_{DU}) are calculated from the equation

$$R = \frac{\rho_c l}{A}$$

where R is resistance in ohms, ρ_c is collector resistivity, l is length of current path, and A is the cross-sectional area. Figure 11 shows that A for R_{UD} is just the area of the collector contact. Therefore

$$A = (3.4)(0.7) + (0.5)(3.6) = 4.2 \text{ mil}^2 = 2.7 \times 10^{-5} \text{ cm}^2$$

From Figure 11, we find $l = 5 \mu\text{m}$ and $\rho_c = 0.2 \Omega\text{-cm}$. Therefore, the resistance is

$$R_{UD} = \frac{(0.2)(5 \times 10^{-4})}{2.7 \times 10^{-5}} \approx 4 \Omega$$

Similarly, in the calculation of R_{DU} A is the area of the emitter and $l = 5 \times 10^{-4} \text{ cm}$. Therefore the down-up resistance

$$R_{DU} = \frac{(0.2)(5 \times 10^{-4})}{1.8 \times 10^{-5}} \approx 4.4 \Omega$$

The resistance through the buried layer (R_{across}) is a function of the sheet resistivity of the layer measured in ohms/square. The number of squares involved is the length of the current path divided by the width. For example, in Figure 12 the number of squares is three.

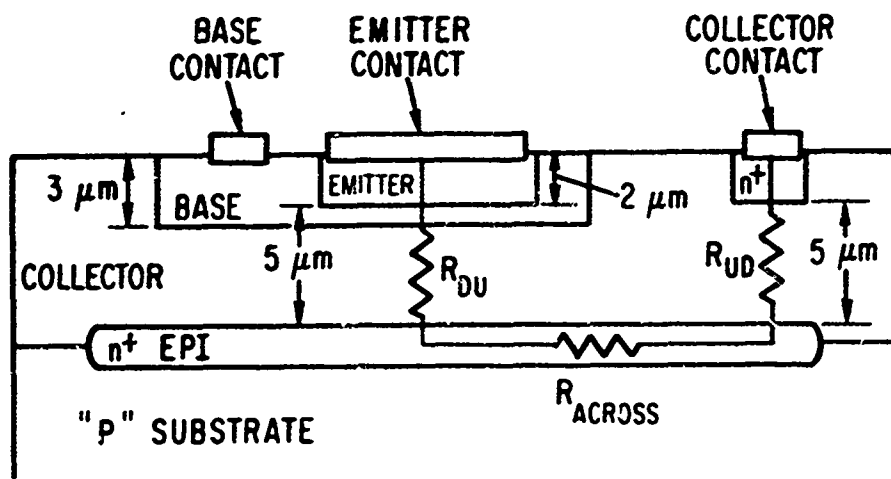
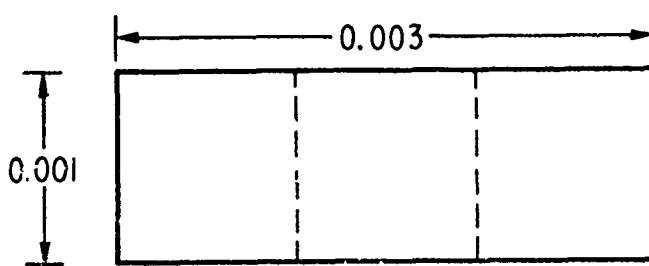


Figure 11. The Three Contributions to the Bulk Resistance of a Transistor



$$\text{No. OF SQUARES} = \frac{\ell}{w} = \frac{0.003}{0.001} = 3$$

Figure 12. Sample Calculation of Number of "Squares"

For our circuit, the width of the current path varies. The width chosen is the average value of the width, as seen in Figure 10. The length can also be determined from Figure 10. Therefore, the resistance is

$$R_{\text{across}} = 3(\Omega/\text{square}) \times \frac{(1 \text{ mil})(\text{square})}{(2.3 + 2.1) \text{ mil}} = \frac{3}{4.4} \approx 1 \Omega$$

The total resistance of the transistor is therefore

$$R_{\text{BULK}} = R_{UD} + R_{\text{across}} + R_{DU} = 4 + 1 + 4.4 = 9.4 \Omega$$

The resistance of the aluminum metallization leading from the output transistor to ground is

$$R_{\text{MET}} = \frac{\rho l}{A} = \frac{(2.82 \times 10^{-6} \Omega\text{-cm})(0.1 \text{ cm})}{(1 \mu\text{m})(10 \mu\text{m})} = 1.4 \Omega$$

$$\therefore R_{\text{Total}} = R_{\text{BULK}} + R_{\text{MET}} = 9.4 + 1.4 \approx 11 \Omega$$

Having computed the limiting resistance of the current path, we can determine the power dissipated in the junction from Eqs. (A. 1) and (A. 2). The power dissipated in the device is shown in Figure 13. The power per unit area necessary to burn out a junction in a given time can be obtained from Figure 1. With the area of the emitter junction, $1.8 \times 10^{-5} \text{ cm}^2$, known, one can compute the power necessary to burn out the junction for a specific pulse width and from Figure 13 can then find the voltage necessary to cause this burnout. This result is shown in Figure 5. The actual effect of the pulse can be seen with the aid of a microscope. In the case just treated, the pulse burned a path from the emitter to the collector of the output transistor (see Figure 14).

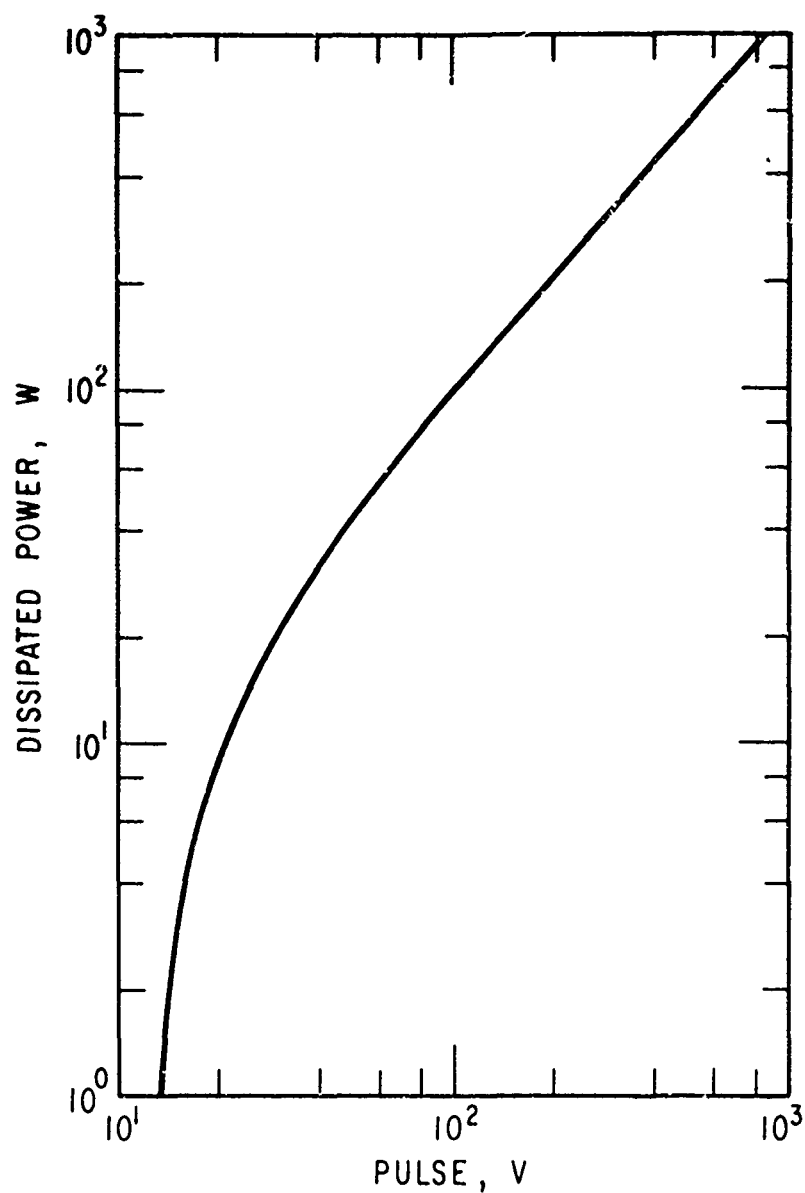


Figure 13. Power Dissipated Across Junction of Output Transistor of Amelco 6041 Dual Three-Input Nand Gate with High-Power Pulser on Output Connection

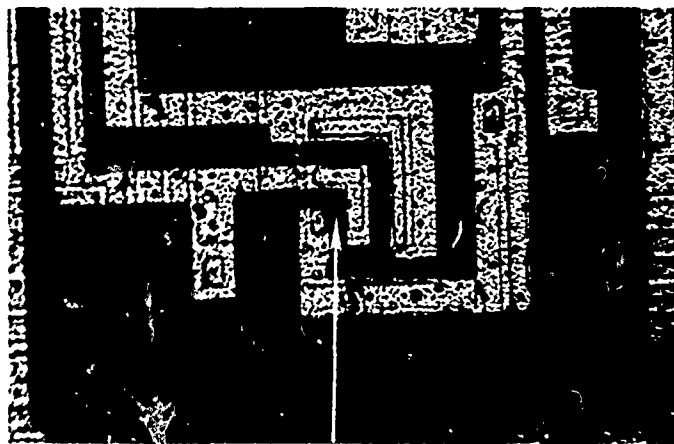


Figure 14. Photomicrograph of Burned-Out
Fairchild 9046 Output Transistor
Caused by Pulses Applied
to Output

APPENDIX B. WUNSCHE CELL CALCULATIONS FOR A PULSE
ON THE INPUT OF AN AMELCO 6041 NAND GATE

The circuit diagram and a photomicrograph of the 6041 are shown in Figures 15 and 16. The areas of the junctions and metallization can be measured from the photomicrograph. For a pulse on the input, the current will flow through input diode D₁ and transistors T₁, T₂, and T₃ to ground. The other possible paths all have limiting resistors and thus can be excluded. It is necessary, therefore, to compute the bulk resistances of D₁, T₁, T₂, and T₃.

The resistance of the input diode is

$$R_{UD} = \frac{\rho l}{A} = 100 \Omega$$

where A is the area of the collector contact

$$R_{across} = \text{sheet resistance} \times \text{number of squares} = 8 \Omega$$

$$R_{DU} = \frac{\rho l}{A} = 45 \Omega$$

where A is the area of the base contact

$$R_{D1} = R_{UD} + R_{across} + R_{DU} = 153 \Omega$$

The resistance of T₁ and T₂ is

$$R_{T1} = \text{sheet resistance} \times \text{number of squares} = 47 \Omega$$

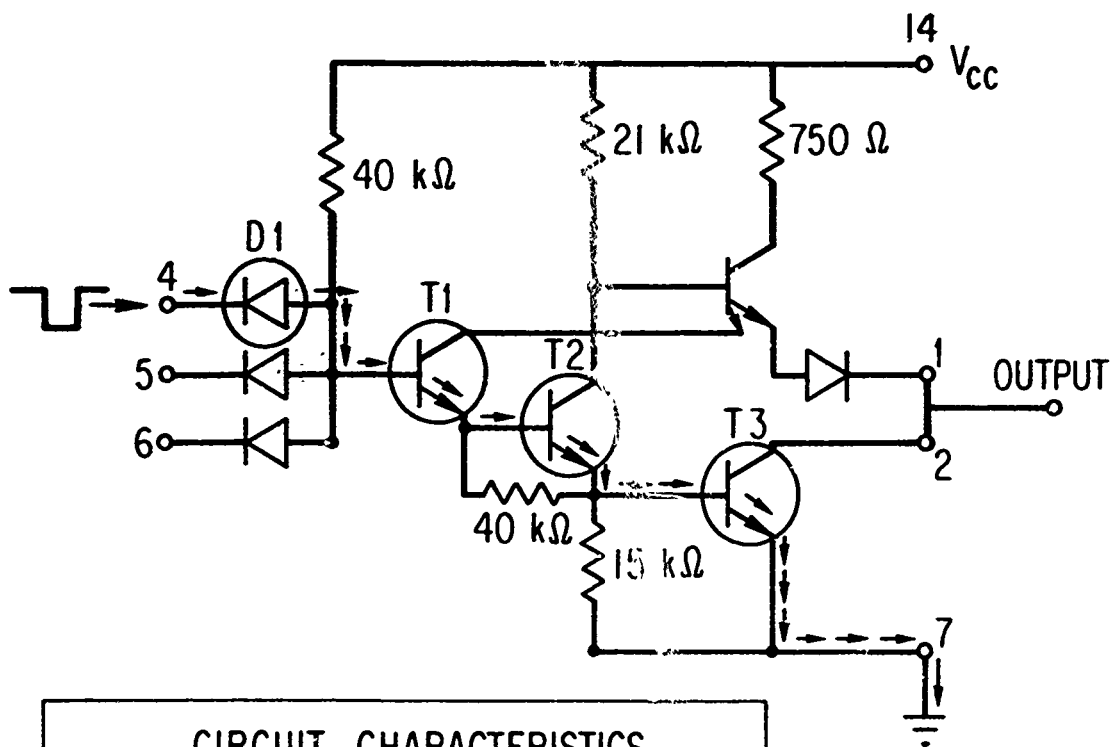
$$R_{T1} = R_{T2} = 47 \Omega$$

The resistance of T₃ is

$$R_{T3} = \text{sheet resistance} \times \text{number of squares} = 50 \Omega$$

The resistance of the aluminum metallization is R = 1 Ω. The total resistance is

$$R_T = R_{D1} + R_{T1} + R_{T2} + R_{T3} + R_{Al} = 297 \Omega$$



CIRCUIT CHARACTERISTICS

BV_{CEO} = 8 V MIN.; 12-15 V TYPICAL

BV_{EBO} = 6 V MIN.; 7-8 V TYPICAL

BV_{CBO} = 40 V MIN.; 50 V TYPICAL

Figure 15. Circuit Diagram for One Channel of Amelco 6041
Dual Three-Input Nand Gate

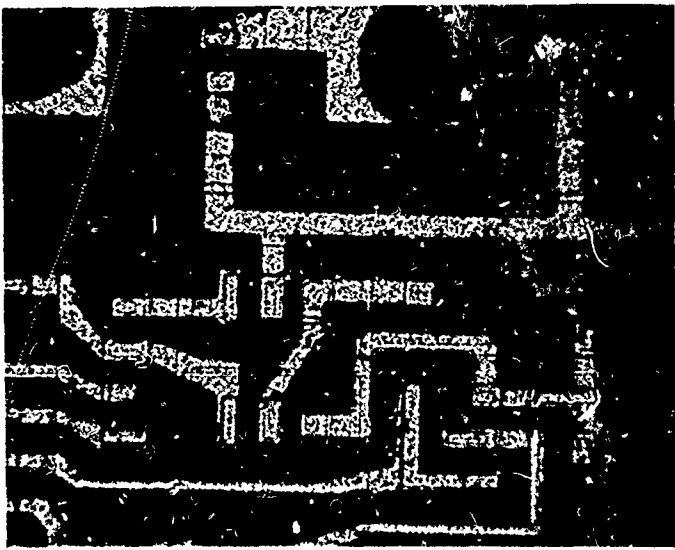


Figure 16. Photomicrograph of Amelco 6041
Nand Gate Geometry

Burnout of the various active elements depends upon the polarity of the pulse delivered to the input. For positive pulses, most of the power is dissipated across the input diode, and it will be most likely to burn out. For negative pulses, the input diode is forward biased and does not dissipate much power. Therefore, most of the power will be dissipated in the transistors T₁, T₂, and T₃. Since T₁ and T₂ have smaller areas than does T₃, transistors T₁ and T₂ are most likely to burn out. For a negative pulse, the current is

$$I = \frac{V}{R} = \frac{V - 3BV_{\text{transistor}}}{297} \quad (\text{B.1})$$

The power dissipated in the junction of T₁ and T₂ is

$$P = IV + I^2 R_{\text{BULK}}$$

Here the power dissipated in the bulk resistance is included because the base is so near the emitter junction. The power is shown in Figure 17. From Figure 16, we can measure the area of the emitter for transistors T₁ and T₂ ($4.3 \times 10^{-6} \text{ cm}^2$). With this value known, we can apply the Wunsch-Bell theoretical values from Figure 1 to obtain a graph of breakdown voltage vs pulse width, Figure 6. The damage mechanism is junction burnout of transistors T₁ and T₂, which can be clearly seen in Figure 18. If the pulse is sufficiently large, D₁, T₁, T₂, and T₃ will all burn out, as is shown in Figure 19.

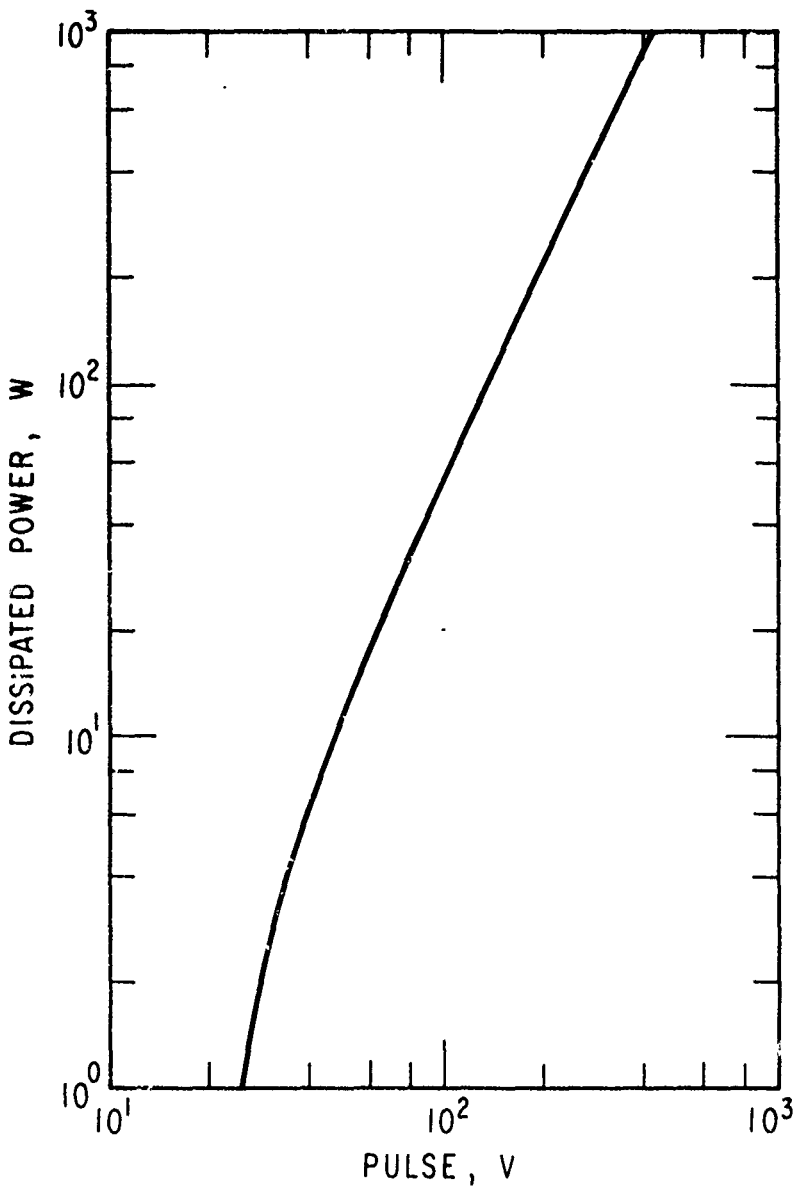


Figure 17. Power Dissipated at Emitter Junction
of Transistor T1 or T2 of Amelco 6041 Nand
Gate with Negative High-Power Pulses
on Input

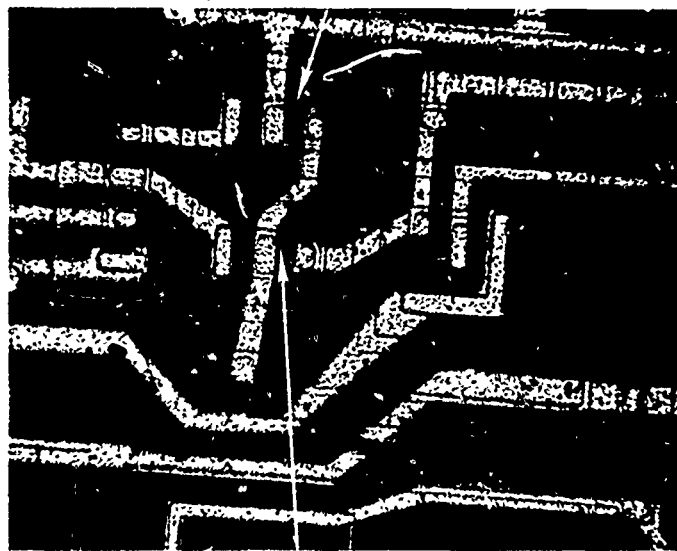


Figure 18. Photomicrograph of Amelco 6041
Nand Gate After Application of High-Power
Negative Pulse to Input, Showing
Failure of Transistors T1 and T2

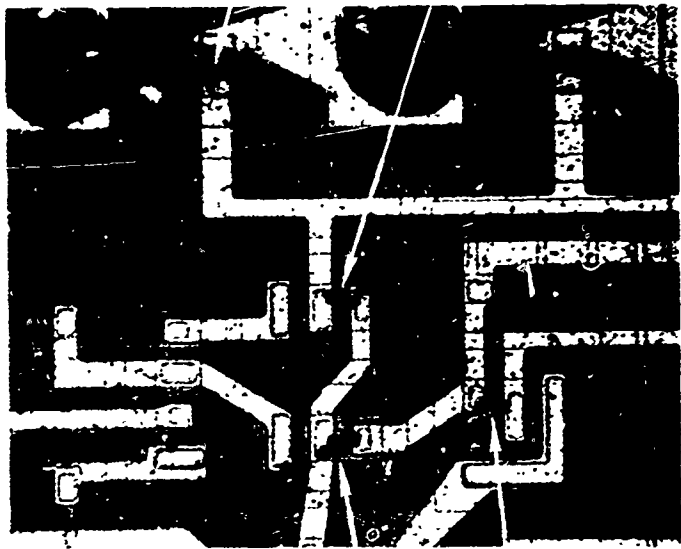


Figure 19. Photomicrograph of Amelco 6041
Nand Gate After Application of High-Power
Negative Pulse to Input, Showing Failure
of Diode D1 and Transistors
T1, T2, and T3